# Assessment of the Mechanical Properties of a new 3D Woven Fibre Composite Material

Fredrik Stig, Stefan Hallström

# Accepted Manuscript


Assessment of the Mechanical Properties of a new 3D Woven Fibre Composite Material

Fredrik Stig, Stefan Hallström

PII: S0266-3538(08)00179-6
DOI: 10.1016/j.compscitech.2008.04.047
Reference: CSTE 4069

To appear in: *Composites Science and Technology*

Received Date: 21 December 2007
Revised Date: 24 April 2008
Accepted Date: 30 April 2008

Please cite this article as: Stig, F., Hallström, S., Assessment of the Mechanical Properties of a new 3D Woven Fibre Composite Material, *Composites Science and Technology* (2008), doi: 10.1016/j.compscitech.2008.04.047

# Assessment of the Mechanical Properties of a new 3D Woven Fibre Composite Material

Fredrik Stig and Stefan Hallström *

*Royal Institute of Technology (KTH)*

*Teknikringen 8, SE 100 44 Stockholm, Sweden*

**Abstract**

Fully interlaced 3D fabric is produced by a new weaving technology, and it is here utilised to produce woven carbon fibre preforms, which are then used as reinforcement in composite materials. The purpose of this study is to assess the mechanical performance of this new type of composite material. A prototype loom was used to weave preforms with a rectangular cross section where all warp and weft yarns were fully interlaced in plain weave. Tensile, compressive, out-of-plane, shear and flexural properties of the composite flat-beam specimens were tested. The in-plane stiffness and strength were found to be lower, while the out-of-plane properties were higher compared to conventional 2D laminates. In terms of strength, it was not possible to quantify the difference, since the specimens with 3D woven material exhibited other failure modes than those tested for.

*Key words:* 3D Woven, Textile composites, Mechanical properties

* Corresponding author
*Email address:* stefanha@kth.se (Stefan Hallström).
*URL:* www.lightweightstructures.se (Stefan Hallström).

## 1 Introduction

Fully interlaced 3D fabric comprising carbon fibres have the potential of changing the way composite structures are designed and built. Aircraft manufacturers are using more and more composite materials in their efforts to reduce weight as exemplified by March [1]. The 3D woven composite preforms offer new fibre architectures and shapes for composite design. According to Khokar [2] the fully interlaced yarns in a network structure increase the structural integrity, and thereby reduce the risk of delamination, and a more effective load transfer can be achieved. There is also a possibility to place more yarns where needed, to tailor the material for specific load cases. Tong et al. [3] argues that there are many benefits with 3D woven composites, for instance increased through-thickness mechanical properties, lower manufacturing cost and improved impact damage tolerance.

This paper presents a first attempt to measure and evaluate the mechanical properties of truly 3D woven fibre composites, according to the definition and principle of 3D weaving set forth by Khokar [4–6]. Khokar argues that 3D weaving must incorporate a dual direction shedding operation, and defines 3D weaving as *"the action of interlacing a grid-like multiple-layer warp with sets of vertical and horizontal wefts"*. The 3D-weaving method uses dual direction shedding operations and produces a fully interlaced structure. It is possible to weave net shaped beams with various types of cross sections for instance: open, closed, solid and thin walled cross sections and it is even possible to weave curved beams, see Fig. 1a. There are possible benefits and drawbacks with a 3D-woven fibre composite, both on a structural and a material level. The technology offers the freedom to produce many desired cross sectional

shapes and weave patterns. It is possible to engineer the mechanical properties by changing weaving parameters like number of warp and weft yarns, yarn tension, warp and weft yarn types and tow sizes and thereby tailoring the fibre volume fraction in different directions .

## 2 Approach

The purpose of this study was to extract constitutive parameters and material strengths for the 3D-woven fibre composite on a material level, and compare the results with corresponding properties of three more conventional material concepts; (i) 2x2 twill, (ii) non-crimp $[0\ 90]_{3s}$ and (iii) non-crimp $[90\ 0]_{3s}$. To do so, flat beam specimens with a rectangular cross section were manufactured and tested. The performed work was constrained by limitations in size, and semi-manual production of the 3D preforms. The four different configurations are here referred to as "3D", "Twill", "NC-0" and "NC-90", respectively, see Fig. 2 for illustration. Fig. 1b shows the 3D-woven reinforcement woven in the prototype 3D-weaving loom. It consisted of 3 rows of warp yarns wherein each row had 16 warp yarns (W), two rows of straight stuffer warp yarns (S) with each row having 15 yarns, 16 vertical weft yarns (VW) and 3 horizontal weft yarns (HW). The structure of the 3D-weave is schematically illustrated in Fig. 3. As opposed to warp yarns, stuffer yarns have no or little crimp since they are not interlaced with weft yarns. Their presence in the weave is optional and contributes to longitudinal stiffness and enhanced fibre volume fraction in the warp direction. The stuffer yarns also increase the total fibre volume fraction since their presence enhances the packing of the yarns.

The woven preforms were impregnated with vinyl ester resin by vacuum injec-

tion moulding in a semi-soft mould to form composite flat beam specimens. The three 2D laminates made for comparison were also manufactured using vacuum infusion. The same fibre type (Toray T700 12k) and resin (Reichhold Dion 9500 vinyl ester) were used in all four material types. The areal fibre weight was approximately the same in all specimens, but due to the differences in fibre structure, the thickness, and thus the fibre volume fraction of specimens with different reinforcement varied to some extent. For the same reason, the fibre distribution percentage, $DP$, between different directions also varied between the different fabric structures, as indicated in Table 1, wherein the thickness ($t$) and fibre areal weight of each material are also presented. The fibre volume fractions were calculated based on measured weights and dimensions of constitutive materials. The variation of thickness for the 3D specimens was due to use of a semi-soft mould, and the variation in areal fibre weight was probably a consequence of the somewhat irregular weave pattern due to the semi-manual production in the prototype weaving machine. The tensile, compressive, out-of-plane, shear and flexural properties of the four materials were tested and the results compared. In this work the longitudinal direction is denoted by 1, the transverse direction by 2 and the out-of-plane direction by 3. The study was constrained by limited access to 3D preforms, both in size and quantity. Due to this, some results are more indicative than explicit.

## 3 Experiments

All experiments were performed identically for all four material configurations. Unless otherwise specified, five specimens per material and experiment were

tested at room temperature.

### *3.1 Tensile test*

The tensile tests were performed using ASTM D3039 [7] and the load was measured with an Instron 4505 test machine with a 100 kN load cell. The strains were measured independently from load and without contact with the test specimens using a GOM Aramis 1.3 Digital Image Correlation (DIC) equipment for three of the laminates (NC-0, Twill and 3D). The purpose of using the DIC equipment was to be able to measure not only the in-plane strains and hence the in-plane Poisson's ratio but also the out-of-plane displacement. The latter were used to calculate the out-of-plane strains in order to obtain the out-of-plane Poisson's ratio. To compensate for any out-of-plane rigid body motions, one DIC system on each side of the specimen was used. The longitudinal strain in the NC-90 specimens was measured with strain gauges instead of the DIC-system. The recommended specimen thickness according to the ASTM D3039 standard is 2.5 mm, but the thickness of the Twill specimens was only 2.2 mm. However, it has been shown in experimental work by Sun Piu Ng et al. [8] that a thickness of 1.31 mm is sufficient for 2x2 twill when using the ASTM 3039 standard.

### *3.2 Compression test*

The ultimate compressive strain was measured using ASTM D3410 with a test fixture according to procedure B [9]. An Instron 4505 test machine with a 100 kN load cell was used to measure the compressive force, and the strain was

measured using two strain gauges (one on each side of the specimens) of the type Showa N11-FA-5-350-11.

### *3.3 Out-of-plane strength test*

The out-of-plane strength was measured with a non-standardized test procedure. The material was adhesively bonded between two aluminium cylinders which were fitted in a test-rig, see Fig. 4. The test specimens were coin shaped with a diameter of only 20 mm, due to the limited width of the 3D-woven material. A Teflon spacer was used to ensure that no adhesive bridging occurred between the cylinders. A 30 kN load-cell was used to measure the load in an Instron 556x 30 kN test machine.

### *3.4 Short beam shear*

The inter-laminar shear strength (ILSS) was tested using the CRAG short beam shear test [10]. The geometry of the test coupons differed somewhat from the standard for a number of reasons. Firstly, according to the standard the span length and the coupon width are functions of the coupon thickness which for the four different materials varied between 2.2 and 3.2 mm. Secondly, only a few different span lengths could be used in the short beam shear rig. The diameters of the support-roller and the loading-nose were 6 and 10 mm respectively, and the span length was 17.5 mm. Again the Instron 556x 30 kN test machine was used together with a 30 kN load-cell. The short beam shear test measures the ILSS as "$0.75P/A$", where $P$ is the loading-nose force and $A$ the cross section area. However, the stress field is affected by the short distance

between the supports and therefore ILSS is not a measurement of pure shear strength. Nevertheless, the test is meaningful for comparative studies. Since the results only were to be compared, the same span length and the same beam geometry (except for thickness) were used.

### *3.5 Flexural test*

The shear stiffness $G_{13}$ was obtained by first measuring the bending stiffness $D$ and the shear stiffness $S$ using the ASTM D790 three point bending test [11]. The span length in the test standard is set to minimise shear deformations, but here a number of different shorter span lengths were used in order to determine the shear stiffness as well. An Instron 556x 30 kN test machine equipped with a 500 and a 5000 N load cell was used. The deflection under the loading nose was measured with a digital displacement device. One specimen of each material type was tested using 13 different span lengths ranging from 50 mm to 180 mm. The load and displacement data were used to calculate the bending and shear stiffness. The method uses the fact that the deflection under the loading nose, $w$, in three-point bending can be expressed as

$$w = w_b + w_s = \frac{PL^3}{48D} + \frac{PL}{4S}, \tag{1}$$

where $P$ is the load under the loading nose, and $L$ is the span length. The shear part of the total deflection is denoted $w_s$ and the bending part $w_b$. An over-determined equation system was set up using test results (loads and deflections) from the 13 different span lengths. The system was then solved using a least square algorithm. The out-of-plane shear modulus, $G_{13}$, was then calculated from the definition of shear stiffness, $S$, in first order shear

deformable beam theory, according to

$$G_{13} = \frac{S}{A_s}, \tag{2}$$

where $A_s = A/\beta$. The cross section area is denoted $A$, and the parameter $\beta$ equals 1.2 for a rectangular cross section.

## 4 Results and Discussion

The different fabric structures complicated comparison of constitutive and strength parameters between the material types; therefore, the failure behaviour is here also emphasised and discussed. To the benefit of the 3D-woven composite it is not known whether its non-smooth surface had any negative effect on the strength results.

### *4.1 Tensile test*

The tensile test results are listed in Table 2 and stress-strain curves together with images of failed specimens are presented in Fig. 5. All Young's-moduli are evaluated between 0.2 and 0.3 % strain. Since all materials have similar fibre areal weight the difference in thickness mainly reflects a difference in the amount of matrix in the composites, and lower thickness hence yields a correspondingly higher fibre volume fraction and modulus. Thus, in order to make comparison meaningful, the moduli are first normalised with respect to the fibre content in the 1-direction, $v_{f,1}$, and then then normalised again with

respect to the results for the NC-0 material, according to

$$E' = \frac{E}{v_{f,1}} \qquad and \qquad E'' = \frac{E'}{E'_{NC-0}}. \tag{3}$$

The stress-strain curves for the Twill, see Fig. 5b, illustrate a distinct momentary elongation around $\sigma_1 = 350 - 400$ MPa. At this stage cracking noises were heard during testing. It is believed that the tensile load forced the originally crimped warp yarns to straighten. Such straightening is predominantly prevented by the matrix which eventually fails. Straightening of yarns ought to result in stiffening of the material. However, in this case it is associated with matrix damage and presumably also some fibre damage. The stiffening effect of yarn interlocking is also reduced when the matrix fails, making the overall effect on the stiffness harder to predict. In the experiments the stiffness dropped slightly after the hump. The failure is illustrated in the top left corner of Fig. 5b. The DIC-data revealed that at the hump in the stress-strain curve, the thickness of the laminate suddenly increased and the width decreased, supporting the presented argument. The stress-strain curves of the 3D material are more non-linear than those for the other materials, indicating progressive failure. The stuffer warp yarns have little or no crimp and they will contribute more to the stiffness than the interlaced warp yarns. A gradual reduction in stiffness is seen at higher strains, presumably due to matrix cracks. The interlaced structure of the 3D-weave and the presence of stuffer yarns are believed to prevent the sudden abrupt elongation and out-of-plane thickening seen for the Twill. Both the Twill and the 3D materials have crimp, but their respective failure modes are very different; the Twill specimens splinter entirely, whereas the 3D specimens show more localised damage after failure, as seen in Fig 5a and 5b. The non-crimp materials both show relatively linear

behaviour up to failure and also some splitting after failure.

The normalised and non-normalised Young's moduli, ultimate strain, Poisson's ratio and the ultimate force per unit width, $\hat{F}_{1,t}$, are presented in Table 2. The non-normalised Young's-moduli for the two NC materials are in reasonable agreement with the calculated values using classical laminate theory (CLT), which generally overestimates the stiffness. The normalised Young's modulus for the NC laminates are virtually the same. However, the Twill and 3D materials show 14 % and 34 % lower normalised Young's-modulus, respectively, which is likely due to crimp. The warp yarns in the 3D material has more crimp than the yarns in the Twill, but it is difficult to assess the influence of the stuffer warp yarns, which possibly are slightly crimped too. The crimp also influences the ultimate strain, here used as a measure of strength, since all specimens have the same fibre areal weight and the thickness variations made the ultimate stress more dubious to interpret. The Twill has high ultimate tensile strain (if the entire stress-strain curve is taken into account) but in a sense it fails at a considerably lower strain than the other materials. An effect of crimp can be seen in the strain-fields in Fig. 6, wherein the Twill and 3D specimens exhibit higher strain gradients than the NC:s, since the crimp contributes to resin-rich areas on the surface of the specimens. The low in-plane Poisson's ratio of the NC-0 and Twill materials could be due to transverse fibres which prevent lateral contraction, similar to observations made by Ng et al. [8]. The measured Poisson's ratio of the Twill laminate corresponds very well with the experimental and numerical data presented in [8]. It was not possible to measure the strains in the 3-direction because they were too small to detect, and consequently no out-of-plane Poisson's ratios were possible to obtain.

### *4.2 Compression test*

The compression test proved to be more difficult. All test specimens showed acceptable failure behaviour according to the test standard [9], see Fig. 7. However, some tests failed to meet the bending criterion defined as

$$B_y = \frac{|\epsilon_1 - \epsilon_2|}{|\epsilon_1 + \epsilon_2|} \cdot 100 \leq 10\%, \tag{4}$$

where $B_y$ is the percent bending. If a specimen bends during compression, the stress-strain curves from the two opposite sides diverge. For the Twill specimens the two curves are straight but show different slope. One possible reason for this difference is the size of the strain gauges being smaller than the facets in the Twill surface pattern. Since the strain gauge is smaller, the resulting strain is dependent on whether the gauge is mounted on a 90 ° or a 0° yarn, or on some boundary between the two. This is not according to standard but was a trade off between having the same gauge-length, and free span-length for all specimens, and at the same time ensuring that no specimen would bend. The Twill results do not meet the bending criterion even though no bending occurred. Due to this, the Twill results are here regarded as valid. The Young's moduli, which are calculated between 0.05 and 0.1 % strain, the force per unit width $\hat{F}_{1,c}$ and the ultimate strain are shown in Table 3. The different slopes in the Twill's stress-strain curves made evaluation of the modulus of elasticity ambiguous. The mean value was used, and it corresponds well with the Twill's tensile modulus. The NC materials exhibited 10-14 % difference in Young's-moduli between the compressive and the tensile tests, while the results for the 3D material were very consistent. The ultimate strain for the NC specimens was more than twice as high as for the Twill and the

3D specimens. This could again be attributed to the crimp. The 3D material showed even lower compressive strength than the Twill. The question remains how the stuffer yarns influence the compressive strength. The compressive failure mode of all material types can be seen in Fig. 7, note that the failure in the 3D specimens occurs at an angle with respect to the 2-axis. This failure pattern is unique for the 3D specimens, and is believed to be related to in-plane crimp. The NC specimens all showed a brooming failure mode, according to ASTM D3410 [9]. The Twill failure mode was through-thickness fibre failure, and in a few specimens also at an angle in the 1-3 plane.

### *4.3 Out-of-plane strength test*

The out-of-plane test was not expected to reveal the true out-of plane strength of the 3D material since the adhesion between the 3D specimens and the aluminium cylinders was expected to be weaker than the 3D material. The limitations in specimen size also prevented any other type of test in this study. All tests with 3D specimens and a few of the others showed adhesion failure between the adhesive layer and the aluminium cylinders. Table 4 presents the results. Only test specimens that failed in delamination are included in Table 4. For this test there was no difference between the non-crimp laminates and they are consequently presented together. The highest measured out-of-plane stress for the 3D specimens before adhesive failure was 18.2 MPa, which is between 22 and 40 % higher than the out-of-plane strength of the 2D-laminates. However, the question remains how high the out-of-plane strength of the 3D-laminate's is. The out-of-plane strength for the non-crimp laminates was the same as for the Twill. Note that the bonding quality of the 3D specimens were higher than

for the NC specimens which failed adhesively. The delamination failure mode of the Twill and the adhesive failure of the 3D specimens can be seen in Fig. 9.

### *4.4 Short beam shear*

In the short beam shear test both non-crimp laminates failed in shear. The Twill failed in shear but also showed crushing damage under the loading nose. The 3D specimens all failed in crushing which made comparison with the other materials dubious. The shear stress when crushing occurred is however also presented, in Table 4. The shear strength of the 3D material is higher than the presented ILSS which in turn is 37-65 % higher than the ILSS for the traditional 2D weaves. The reason for this increase in shear strength could likely be attributed to the weft yarns in the 3-direction, which constitute about 6 % of the distribution percentage $DP$, see Table 1. However, the term ILSS is not applicable for the 3D material with fully interlaced yarns because it is not composed of separate lamina layers. The difference in failure mode is in correspondence with work done by Mohammed et al. [12], who reported that a fibre content of a few percent in the 3-direction increases apparent ILSS by 10-33 % compared to traditional woven 2D-materials.

### *4.5 Flexural test*

Assuming beam theory being valid, the resulting bending and shear stiffness, and shear moduli from the 3-point bending test are shown in Table 5. The calculated bending stiffness $D$, using CLT, was significantly higher than the

measured ones. The reason for this is likely that the tested materials have thin matrix-rich layers on the top and bottom surfaces of the specimens, from the resin infusion process. The CLT does not take this into account and the stiffness is therefore over-predicted. The shear stiffness is not only a material property but also depends on the loading condition and the geometry according to Hayes [13], and should thus be interpreted with that in mind. As there is no obvious way to normalise the shear modulus to account for differences in thickness, fibre architecture and fibre volume fraction, the non-normalised values are presented in Table 5.

## 5 Conclusion

Generally the 3D woven material has higher out-of-plane properties and lower in-plane properties compared with the more traditional 2D-laminates. The experiments suggest that both the out-of-plane tensile strength and shear strength are higher for the 3D material than the rest. However it was not possible to quantify the difference since the sought modes of failure never occurred in the 3D material. A different type of test is needed to measure the 3D materials' true out-of-plane properties. The results further indicate that crimp has a large effect on the stiffness and strength properties. The 3D and Twill specimens both showed lower normalised in-plane stiffnesses and compressive strength than the NC specimens. The crimp in the Twill laminate caused premature tensile failure since the load acted to straighten the fibre yarns to such an extent that the matrix failed. No such failure occurred for the 3D specimens, in spite of crimp. Presumably it was inhibited by the vertical weft yarns. In compression both woven materials showed lower ultimate strain

than the NC. Adding fibres in the out-of-plane direction affects the failure modes. In short beam shear the failure mode shifts from interlaminar shear failure to crushing under the loading nose. The 3-dimensional crimp in the 3D specimens introduces a new failure mode in compression; the compressive fibre failure occurs at an angle with respect to the 2-axis, most likely due to in-plane crimp.

## 6 Acknowledgement

The authors would like to thankfully acknowledge Dr. Nandan Khokar, Biteam AB, Sweden, for generously assisting with the production of woven 3D samples, and Chelton Applied Composites, Sweden, for supplying carbon fibre roving. This work has been financially supported by the European Commission through the MOJO project (FP6 contract no AST5-CT-2006-030871 MOJO).

## References

[1] G. Marsh, Airframers exploit composites in battle for supremacy, Reinforced Plastics 49 (3) (2005) 26–32.

[2] N. Khokar, Suitability of 3D-weaving process for producing advanced pre-forms for modular structrual elements, in: Proceedings of the 27th SAMPE Europe Conference, Paris, 2006.

[3] L. Tong, A. Mouritz, M. Bannister, 3D Fibre Reinforced Polymer Composite, Elsevier, 2002.

[4] N. Khokar, 3D fabric-forming process: Distinguishing between 2D-weaving,

3D-weaving and an unspecified non-interlacing process, Journal of the Textile Institute 87 (1) (1996) 97–106.

[5] N. Khokar, 3D-weaving: Theory and practice, Journal of the Textile Institute 92 (1) (2001) 193–207.

[6] N. Khokar, Noobing: A nonwoven 3D fabric-forming process explained, Journal of the Textile Institute 93 (1) (2002) 52–74.

[7] ASTM D 3039-00, Standard Test Method for Tensile Properties of Polymer Matrix Composite Materials, American Society for Testing and Materials ,100 Barr Harbour Drive, West Conshohocken, PA, United States (2000).

[8] S.-P. Ng, P.-C. Tse, K.-J. Lau, Numerical and experimental determination of in-plane elastic properties of 2/2 twill weave fabric composites, Composites: Part B 29 (6) (1998) 735–744.

[9] ASTM D 3410-95, Standard Test Method for Compressive Properties of Polymer Matrix Composite Materials with Unsupported Gage Section by Shear Loading, American Society for Testing and Materials,100 Barr Harbour Drive, West Conshohocken, PA, United States (1995).

[10] P. Curtis, Crag test method for the measurement of the engineering properties of fibre reinforced plastics, Technical report 88012, Royal Aerospace Establishment (1988).

[11] ASTM D 790-99, Standard Test Method for Flexural Properties of Unreinforced and Reinforced Plastics and Electrical Insulating Materials, American Society for Testing and Materials,100 Barr Harbour Drive, West Conshohocken, PA, United States (1999).

[12] M. H. Mohamed, A. E. Bogdanovich, L. C. Dickinson, J. N. Singletary, R. B. Lienhart, A new generation of 3D woven fabric preform and composite, SAMPE Journal 37 (3) (2001) 8–17.

[13] M. D. Hayes, Structural analysis of a pultruded composite beam: Shear stiffness determination and strength and fatigue life predictions, Ph.D. thesis, Virginia Polytechnic Institute and State University, Blacksburg, Virginia (November 2003).

(a) (b)

Fig. 1. (a) 3D-woven beams with different cross sections. (Courtesy of Biteam AB, www.biteam.com) and (b) dry 3D woven preform used in this study.

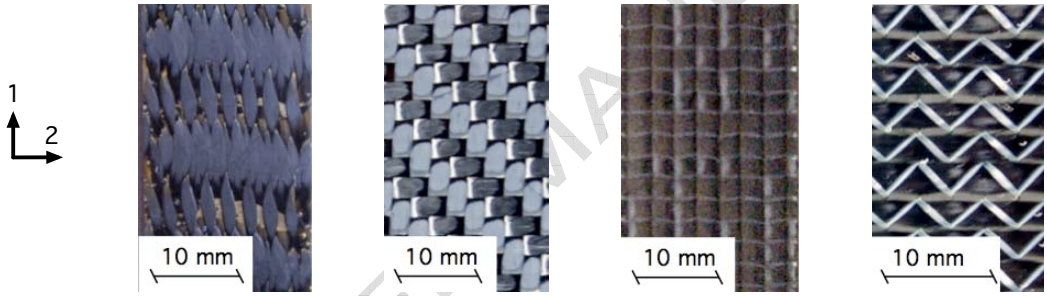


(a) 3D (b) Twill (c) NC-0 (d) NC-90

Fig. 2. Illustration of the tested composite flat beam specimens.

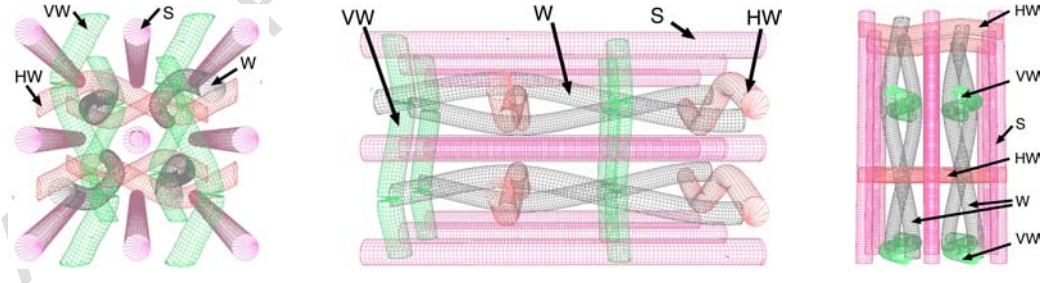


(a) View in 1-direction (b) View in 2-direction (c) View in 3-direction

Fig. 3. Illustrations of the weave pattern in a fully interlaced 3D-weave. The illustrations were made with the software TexGen.

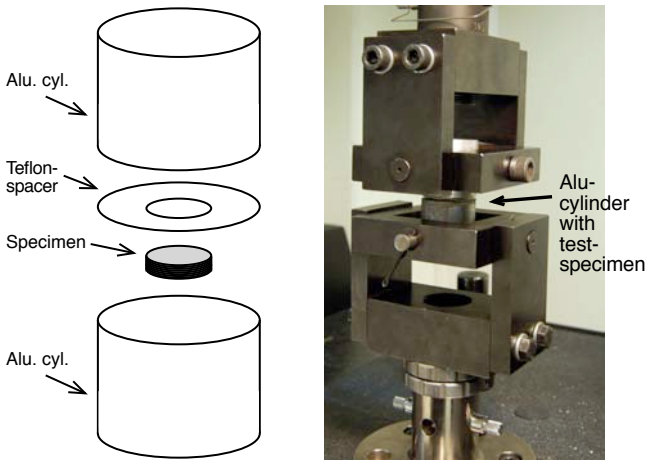


(a) (b)

Fig. 4. The out-of-plane strength test setup, (a) test specimen and (b) specimen in test fixture.

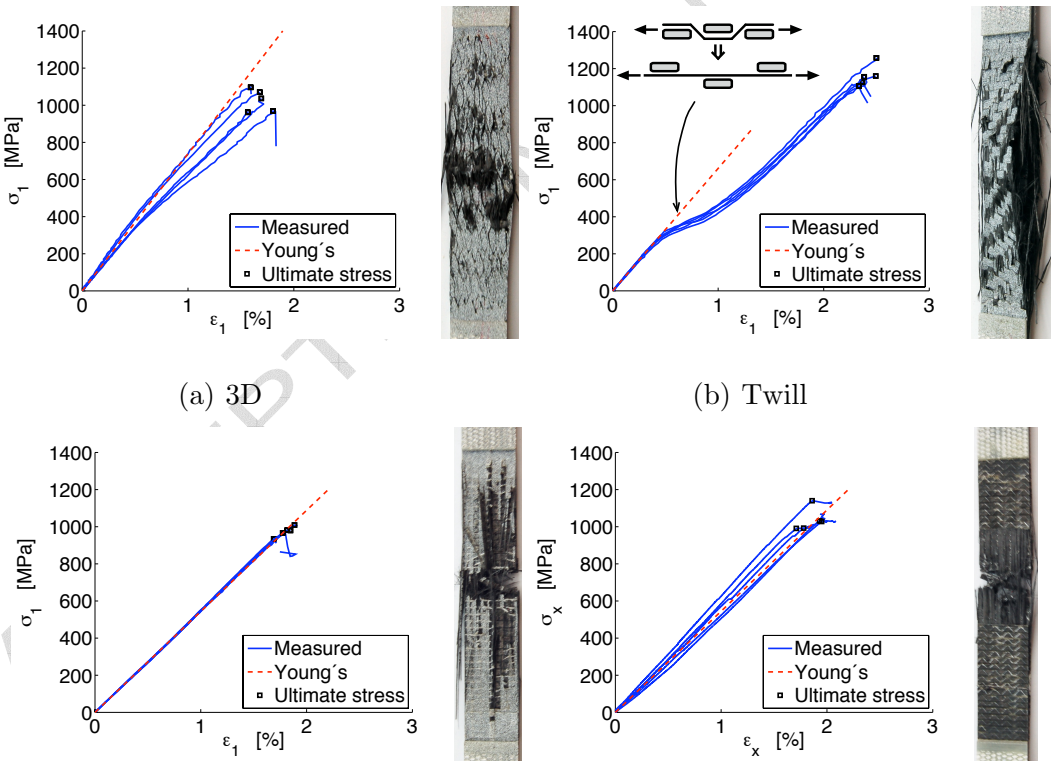


(a) 3D (b) Twill

(c) NC-0 (d) NC-90

Fig. 5. Stress-strain curves for all materials.

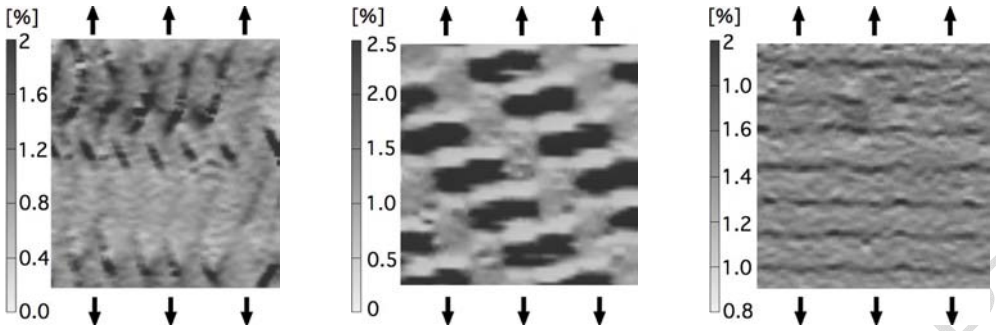


(a) Strain $\epsilon_1$, 3D (b) Strain $\epsilon_1$, Twill (c) Strain $\epsilon_1$, NC-0

Fig. 6. Longitudinal strain field $\epsilon_1$ for the three materials tested with the DIC equipment. The average strain in the samples are 0.8, 1.4 and 1.3 % respectively.

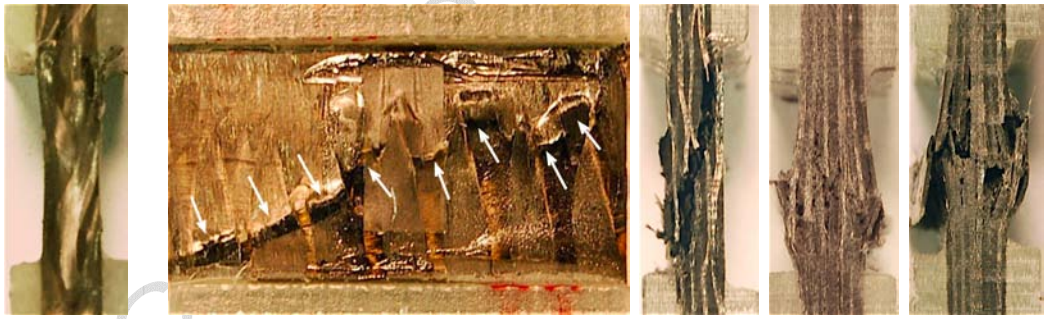

(a) 3D (b) Twill (c) NC-0 (d) NC-90

Fig. 7. Failure modes in compression. (a) The warp yarns in the 3D specimens fail locally at an angle, see the right hand image, (b) fibre failure in the Twill and (c)+(d) brooming fibre failure of the two non-crimp laminates.

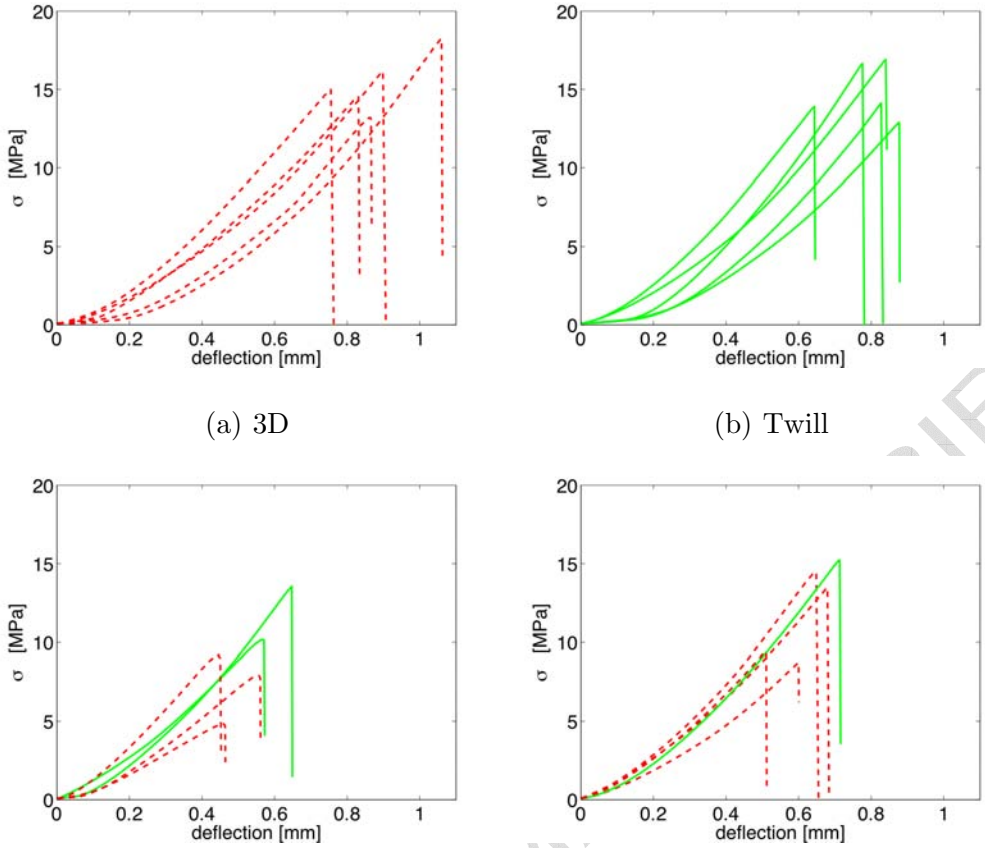


(a) 3D (b) Twill

(c) NC-0 (d) NC-90

Fig. 8. Experimental results from out-of-plane strength test. Dashed lines represents adhesive failure and solid lines delamination.

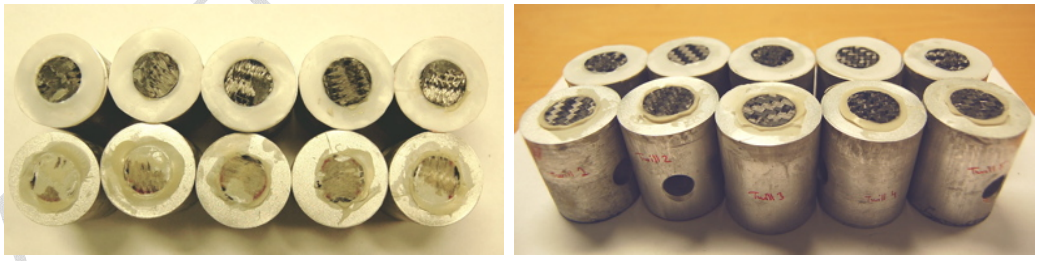

(a) 3D (b) Twill

Fig. 9. (a) The 3D specimens showing cohesive failure and (b) the twill specimens showing clear material failure.

Table 1

Description, notation and lamina properties of the four material types. The distribution percentage $DP$ expresses the percentage of fibres in the 1, 2 and 3-direction respectively.

| Notation | Type | lamina | $t$ [mm] | $\frac{m_{fibre}}{area}$ [ g/m$^2$] | $v_f$[1] | $DP_{(1/2/3)}$[%] |
|---|---|---|---|---|---|---|
| 3D | 3D-woven | N.A. | 2.65-2.9 | 2210-2480 | 0.54 | 86/8/6 |
| Twill | 2x2 twill | 4 layers | 2.2 | 2410 | 0.64 | 50/50/0 |
| NC-0 | Non-crimp | $[0\ 90]_{3s}$ | 3.2 | 2560 | 0.46 | 50/50/0 |
| NC-90 | Non-crimp | $[90\ 0]_{3s}$ | 3.1 | 2540 | 0.47 | 50/50/0 |

Table 2

The measured, calculated and normalized Youngs-modulus, Poisson's ratio, ultimate strain and ultimate force per unit width, $\hat{F}_{1,t}$, from tensile tests. Data are presented as average values and standard deviations, where applicable.

| | $E_1$ [GPa] | $E_{1,CLT}$ [GPa] | $E_1''$ [-] | $\nu_{12}$ [-] | $\hat{\epsilon}_1$ [%] | $\hat{F}_{1,t}$ [$\frac{N}{mm}$] |
|---|---|---|---|---|---|---|
| 3D | 72.6 ± 6.1 | N.A. | 0.66 | 0.333 ± 0.057 | 1.78 ± 0.11 | 2957 ± 135 |
| Twill | 65.0 ± 4.5 | N.A. | 0.86 | 0.039 ± 0.014 | 2.57 ± 0.09 | 2575 ± 111 |
| NC-0 | 54.5 ± 0.7 | 57.0 | 1 | 0.049 ± 0.014 | 1.87 ± 0.10 | 3082 ± 101 |
| NC-90 | 55.0 ± 5.4 | 57.0 | 0.99 | N.A. | 1.85 ± 0.10 | 3259 ± 173 |

Table 3

Results from compression test, average values and standard deviations.

| | $E_{1,c}$ [GPa] | $\hat{F}_{1,c}[\frac{N}{mm}]$ | $\hat{\epsilon}_{1,c}$ [%] | Number of valid tests |
|---|---|---|---|---|
| 3D | 68.7 ± 5.3 | 694± 177 | -0.39 ± 0.06 | 3 |
| Twill | 66.7 ± 7.5 | 588 ± 64 | -0.42 ± 0.07 | 5 |
| NC-0 | 49.2 ± 1.0 | 1508 ± 51 | -0.92 ± 0.06 | 4 |
| NC-90 | 47.9 ± 1.1 | 1579 ± 222 | -1.13 ± 0.22 | 3 |

Table 4

Out-of-plane strength and ILSS. (*Note that the 3D specimens all failed in crushing)

| | $\hat{\sigma}_3$ [MPa] | ILSS [MPa] |
|---|---|---|
| 3D | cohesive failure | 44.3 ± 4.4* |
| Twill | 14.9 ± 1.8 | 26.8 ± 1.2 |
| NC-0 | 13.0 ± 2.6 | 30.4 ± 1.6 |
| NC-90 | | 32.4 ± 1.9 |

Table 5

Bending and shear stiffnesses and shear modulus from bending tests.

| | $D$ [Nm$^2$] | $D_{CLT}$ [Nm$^2$] | $S$ [kN] | $G_{13}$ [GPa] |
|---|---|---|---|---|
| 3D | 1.41 | N.A. | 46 - 50 | 1.0 - 1.1 |
| Twill | 0.94 | N.A. | 45 - 60 | 1.2 - 1.6 |
| NC-0 | 2.87 | 3.6 | 76 - 79 | 1.4 - 1.5 |
| NC-90 | 1.88 | 2.3 | 87 - 93 | 1.7 - 1.8 |